

Adaptive Quantum State Tomography for Arbitrary Single Qubits

Syed Muhammad Kazim, Ahmad Farooq, Junaid ur Rehman,
and Hyundong Shin

Department of Electronics and Information Convergence Engineering, Kyung Hee
University, Yongin-si, 17104 Korea

E-mail: hshin@khu.ac.kr

29 March 2022

Abstract. Several Bayesian estimation based heuristics have been developed to perform quantum state tomography (QST). However, specialized techniques for pure states do not work well for mixed states and vice versa. In this paper, we present an adaptive particle filter (PF) based QST protocol that works efficiently for all single qubit states, due to its unabating perseverance to find the states' diagonal bases. We further identify enduring problems in popular PF methods relating to the subjectivity of informative priors and the invalidity of particles produced by resamplers, and propose solutions. Numerical examples and implementation on IBM quantum devices demonstrate the improved performance for arbitrary qubits and readily applicability of our proposed scheme.

1. Introduction

With increasing research and development in the fields of quantum information and computing, accurate identification and estimation of system components has become vital in efficient operation of practical quantum devices. Quantum state tomography (QST) is one such technique, which is used to characterize an unknown given quantum state ρ . More formally, QST statistically reconstructs a density matrix ρ using data generated by measuring a large number N of identically prepared copies of ρ .

Generally, the reliability and accuracy of the estimated density matrix can be improved by increasing N . Due to the resource-intensive nature of QST, a key figure-of-merit of any QST technique is its scaling with respect to N , which can be improved by measuring ρ in some optimal measurement basis. Therefore, special interest in QST has been given to the development of optimal basis for measurement [1], [2]. Improvement in measurement precision has been experimentally demonstrated when projectors of the eigenstates of Pauli operators employed in standard measurement strategies are supplanted by mutually unbiased bases (MUB) [3]. Despite the success of MUBs, it has been argued that static approaches utilizing a fixed set of measurements do not take

advantage of the information obtained from measurements during QST [4]. Therefore, adaptive realizations of QST are better positioned to reduce redundancy.

It has been shown analytically that the worst-case infidelity can be reduced to $O(1/N)$ if ρ is measured in its diagonal basis [5]. Since ρ is unknown, its diagonal basis is also a priori unknown. Adaptive techniques for QST have been developed in the past decade, which attempt to approach the diagonal basis of ρ and employ it as a measurement basis. For example, popular maximum likelihood estimation (MLE) based adaptive schemes take a two-pronged approach: perform standard tomography on $N/2$ copies of ρ , estimate an intermediate state $\hat{\rho}$, and measure the remaining $N/2$ copies in the diagonal basis of $\hat{\rho}$ [5], [6]. This two-stage tomography using MLE provides improved estimates of ρ for any value of N compared to other standard procedures. However, MLE has inherent issues as a statistical estimator for QST. Although it is possible to reconstruct states using MLE, its incompatibility with error bars makes it difficult to explain the uncertainty and thus the reliability of the estimates. Moreover, as MLE is primarily a frequentist construct, it fits observed frequencies obtained from essentially probabilistic measurements to probabilities [7]. In case of small data sets, MLE can be very unreliable.

Bayesian QST is an alternative to the popular MLE-based QST, which does not suffer from the fundamental drawbacks of MLE. In Bayesian QST, we augment our a priori knowledge of ρ with a data driven likelihood function to produce a well-defined posterior distribution. The posterior distribution allows us to make statistical estimates about ρ and evaluate quantifiable error bars [7, 8, 9]. Moreover, unlike the two-stage MLE, we do not need to know N prior to our experiment.

Adaptive Bayesian schemes have been employed to good effect in QST. Adaptive Bayesian quantum tomography [4] employs a particle filter (PF) based approach, and uses an information-theoretic utility function which optimizes measurements in each iteration. Self-guided quantum tomography (SGQT) [10] is another technique that uses optimization to solve QST for pure states, and has reported considerable improvement in the estimation of pure states. More recently, practical adaptive quantum tomography (PAQT) [11], a hybrid of PF and SGQT, has demonstrated that SGQT can be applied to mixed states with good effect. However, fidelity of SGQT for pure states remain superior. Therefore, despite significant advancements in Bayesian QST, there is still a need for a single technique that is equally adept at estimation of both pure and mixed states. That is, given a random qubit, we should not have to choose between different techniques based on, a difficult to justify, a priori assumption of the state's purity.

In this paper, we present a unified and adaptive practical technique, and report improvements in estimation over existing heuristics for random two-dimensional qubits. Moreover, we also develop a general prior such that the performance of QST is not incumbent on a priori insight of the experiment. Furthermore, we provide a resampling algorithm that corrects the propensity of creating invalid particles of popular resampling techniques. Lastly, we demonstrate the practical nature of the proposed scheme in the estimation of pure and mixed states by providing a proof-of-concept implementation on

IBM's quantum computers [12].

This paper is structured as follows. We delve into the analysis of our prior, explain and provide a pseudocode for resampling of particles, and expound on the functionality of our adaptive protocol in Section 2. We exemplify our protocol in Section 3, and discuss and conclude in Sections 4 and 5, respectively.

2. Methodology

An arbitrary quantum state can be represented by a positive matrix of unit trace, i.e., a density matrix, commonly denoted by ρ . For the case of qubits, ρ can be represented in terms of its Bloch vector \mathbf{r} [13]

$$\rho = \frac{1}{2} (\mathbb{I} + \mathbf{r} \cdot \boldsymbol{\sigma}), \quad (1)$$

where \mathbb{I} is a 2×2 identity matrix, $\mathbf{r} = (r_x, r_y, r_z) \in \mathbb{R}^3$ is a Bloch vector, and $\boldsymbol{\sigma} = (\sigma_x, \sigma_y, \sigma_z)$ is a vector of Pauli operators. Normalization and positivity of ρ translate to the norm constraints on the Bloch vector \mathbf{r} , i.e., $\|\mathbf{r}\|_2 \leq 1$ where $\|\cdot\|_2$ is the Euclidean norm. Throughout this paper, we denote true state and the estimated state by ρ and $\hat{\rho}$, respectively.

2.1. Overview of PF-based QST

The first common step for all QST schemes is to perform measurements on an ensemble of identically prepared copies of ρ . When ρ is measured in configuration $\alpha \in \mathcal{A}$ where \mathcal{A} is a set of informationally complete projective measurement configurations, we observe one of the two possible outcomes $|\psi_\alpha^\ell\rangle$ for $\ell \in \{-, +\}$. Let N_0 qubits be measured in the configuration α , and n_α^ℓ be the number of times we observe the outcome ℓ . Then, the relative frequency $\hat{f}_\alpha^\ell = \frac{n_\alpha^\ell}{N_0}$ approximates the probability of outcome $|\psi_\alpha^\ell\rangle$ defined as $P(|\psi_\alpha^\ell\rangle) = \text{tr}(|\psi_\alpha^\ell\rangle \langle \psi_\alpha^\ell| \rho)$. Then what remains of QST is to best estimate the state $\hat{\rho}$ based on \hat{f} using a statistical method that also specifies the uncertainty of the estimate.

In the QST implementation of Bayesian PF for a qubit [14] [15], we initialize particles $\{\gamma_k\}$ for $k \in \{1, \dots, K\}$ in the Bloch sphere that represent prospective states based on a priori knowledge or some other bias. A particle γ_k is completely described at the t th iteration by its location $\mathbf{r}_k \in \mathbb{R}^3$ and its weight $w_k^t \in \mathbb{R}$. The initial distribution of particles is known as the prior [4], [16]

$$\text{Pr}(\mathbf{r}) \approx \sum_k w_k^0 \delta(\mathbf{r} - \mathbf{r}_k), \quad (2)$$

where $w_k = \frac{1}{K}$. After performing N_0 measurements in α for the t th iteration, we calculate the likelihood [17],

$$\mathcal{L}(\gamma_k | \hat{f}, \alpha) = N_0! \prod_\ell \frac{\text{tr}(|\psi_\alpha^\ell\rangle \langle \psi_\alpha^\ell| \gamma_k)^{N_0 \hat{f}_\alpha^\ell}}{(N_0 \hat{f}_\alpha^\ell)!}, \quad (3)$$

and update the weights of $\{\gamma_k\}$ for the $(t+1)$ th iteration as follows

$$w_k^{t+1} \approx w_k^t \times \mathcal{L}(\gamma_k | \hat{f}, \alpha), \quad (4)$$

where w_k^{t+1} is normalized such that $\sum_k w_k^{t+1} = 1$. The resulting distribution $\{w_k^{t+1}\}$ is the posterior for the t th iteration. Then the Bloch vector of $\hat{\rho}$ is the Bayesian mean estimate (BME) of the distribution, which is simply the weighted aggregate of the posterior

$$\mathbf{r}_{\text{BME}} = \sum_k w_k^{t+1} \mathbf{r}_k. \quad (5)$$

However, PF-based methods suffer from weight collapse where the whole posterior is concentrated on a single particle, giving it all the weight. This situation can be avoided by using an appropriate resampler that effectively reproduces the current distribution when the disparity in the weights of the particles exceeds a predetermined threshold.

In this section, we develop a prior $\text{Pr}(\mathbf{r})$, and identify the inefficiencies of contemporary resampling algorithms and introduce steps to resolve them. We also demonstrate the need and advantages of iterative learning of the set of measurement configurations \mathcal{A} in adaptive Bayesian QST.

2.2. Prior

In Bayesian QST, informative priors [8] can reduce the required number of copies N of ρ in the process. However, the quality of state estimation can suffer if the prior is based on incorrect insight. Although, attention has been afforded to increasing the robustness of protocols which rely on a priori knowledge, this robustness usually means the eventual convergence to the true state [16]. That is, the variance in the required number of samples N to achieve the same infidelity \mathcal{I} for priors of varying authenticity of insight will be substantial. This is a significant problem since in real cases (state tomography of unknown states) where measurement metrics such as infidelity cannot be calculated to ascertain the accuracy of the process at any given stage, there is complete reliance on the statistical model to gauge infidelity for any value of N . Large variances in the output reduce our trust in the model, and hence reduces its practical applicability.

To counter these problems, we need a prior with statistically quantifiable errors. For this purpose, we utilize a small fraction of N to obtain an initial rough estimate of ρ and use a statistical model that specifies our region of interest in the Bloch sphere quantifying our uncertainty in the estimate.

In our protocol, we use a Multivariate Gaussian distribution $\mathcal{N}(\hat{\boldsymbol{\mu}}, \boldsymbol{\Sigma})$ with mean $\hat{\boldsymbol{\mu}}$ and covariance $\boldsymbol{\Sigma}$ as a prior for QST. Initially, we assume no knowledge of the true state ρ . We prepare $3N_0$ copies of ρ where $N_0 \ll N$ and measure Pauli operators $\boldsymbol{\sigma}_j$ for $j \in \{x, y, z\}$ on N_0 qubits each so that n_j^+ (n_j^-) is the number of times we observe the outcome $|\psi_j^+\rangle$ ($|\psi_j^-\rangle$) corresponding to the +1 (-1) eigenstate of Pauli $\boldsymbol{\sigma}_j$. Then the projection that maximizes the probability of the outcomes along $\boldsymbol{\sigma}_j$ is simply $\hat{r}_j = \frac{n_j^+ - n_j^-}{n_j^+ + n_j^-}$

so that $\hat{\boldsymbol{\mu}} = (\hat{r}_x, \hat{r}_y, \hat{r}_z)$ becomes the Bloch vector of the most likely state $\hat{\rho}$ after $3N_0$ measurements. In case $\|\hat{\boldsymbol{\mu}}\|_2 > 1$, we project it onto the surface of the Bloch sphere as a pure state by normalizing it.

To find the covariance matrix of our prior, we must quantify our uncertainty in $\hat{\boldsymbol{\mu}}$. That is, we must find the variance of the sample distribution of our estimate \hat{r}_j , or simply the standard error of r_j for the diagonal elements of $\boldsymbol{\Sigma}$. First, note that the off-diagonal elements of $\boldsymbol{\Sigma}$ are negligible because we perform projective measurements on mutually unbiased bases. Furthermore, since we perform N_0 measurements only, we can use an unbiased estimate of the variance to evaluate the standard error. Then, the i th diagonal entry Σ_{ii} of $\boldsymbol{\Sigma}$ is

$$\frac{n_j^+ (1 - \hat{r}_j)^2 + n_j^- (-1 - \hat{r}_j)^2}{N_0 (N_0 - 1)} + \epsilon,$$

where ϵ is a small constant defined to accommodate all ρ that are eigenstates of our measurement operators. The 3×3 covariance matrix $\boldsymbol{\Sigma}$ is a measure of the variances of the distances of $\hat{\rho}$ from ρ after N_0 measurements in $\boldsymbol{\sigma}$. Furthermore, the diagonal elements of $\boldsymbol{\Sigma}$ are state specific. That is for $\hat{r}_j \rightarrow \{+1, -1\}$, $\Sigma_{jj} \rightarrow 0$ and $\hat{r}_j \rightarrow 0$, $\Sigma_{jj} \rightarrow 0.02$. This state specificity is especially useful for states of high purity since it reduces our volume of interest for the same confidence level.

By utilizing only a fraction of copies, we have accomplished (i) an approximate state that serves as the first step for an adaptive QST technique explained later in the section, and (ii) reduced the region of interest substantially while retaining a statistical description of the uncertainty of our prior. To inspect (ii), let $\hat{\mathbf{r}} = (\hat{r}_x, \hat{r}_y, \hat{r}_z)$, and based on our previous discussion, let each element of $\hat{\mathbf{r}}$ be an independent and identically distributed (i.i.d) Gaussian random variable with $\mathcal{N}(r_i, \sqrt{c_i})$. An ellipsoid can be drawn to represent specific confidence levels using

$$\sum_{i \in \{x, y, z\}} \frac{(\hat{r}_i - r_i)^2}{c_i} = s, \quad (6)$$

where s represents the confidence interval of a χ^2 distribution with 3 degrees of freedom and $s = 11.345$ for a 99% confidence interval. In the case of a maximally mixed state, worst case for our strategy, the diagonal elements of $\boldsymbol{\Sigma}$ are equal, and our ellipsoid corresponds to a sphere with diameter $2\sqrt{cs} = 0.135$. Therefore, compared to an uninformative prior which suggests all valid states are equiprobable, we have reduced the volume of interest by at least 90%. Therefore, by using a ‘just enough’ informative prior which is characterized by its uncertainty works just as well as a good informative prior, and better than one characterized by inaccurate a priori knowledge.

2.3. Resampling

In the PF-based Bayesian estimation, particles have to be resampled when $\sum_{k=1}^{K-1} w_k \approx 0$ and $w_K \approx 1$ [18]. Depending on the resampling algorithm and proximity of the previous

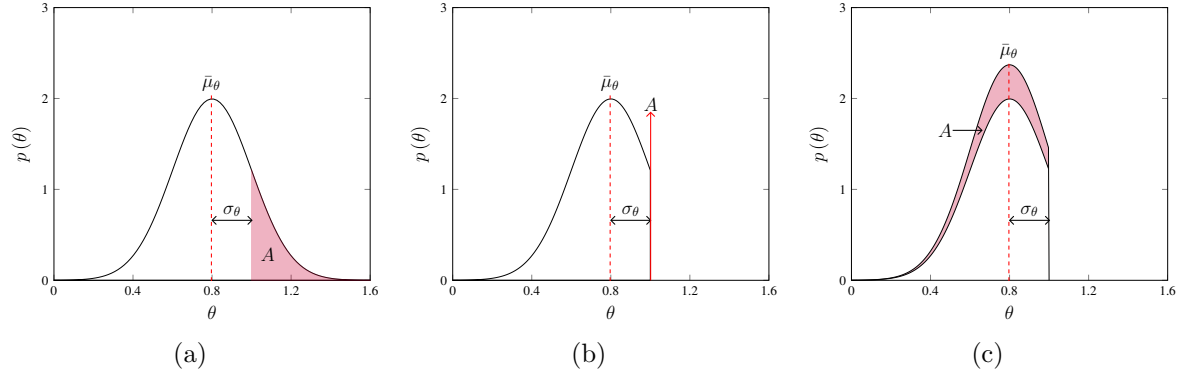


Figure 1. 1-D representation of Bloch sphere where $\theta \in \{X, Y, Z\}$ and $\theta \leq 1$. (a) Resampler with pdf $\mathcal{N}(\bar{\mu}_\theta, \sigma_\theta)$. (b) Output of resampler with concurrent negative eigenvalue truncation schemes morph the pdf such that there is an impulse at $\theta = 1$ of size A . (c) Proposed truncated normal distribution such that the resampler outputs valid states without changing spatial probability ratios of samples.

state to the surface of the Bloch sphere, resampled particles can be invalid states. Invalid states can be visualized as particles not circumscribed by the Bloch sphere, or simply, as states represented by density matrices with eigenvalues less than zero or greater than one. A common workaround is to reduce the negative eigenvalues of such particles to 0, and normalize the remaining eigenvalues to produce valid states [16]. Although this approach is simple, it deforms the resampling distribution and increases computational expense. That is, when a high density of particles are close to the surface of the Bloch sphere (when estimating a pure state, or a state close by), a high number of samples produced after resampling will be invalid states, which are essentially projected onto the Bloch sphere as pure states.

More specifically, suppose that we utilize a univariate Normal distribution $\mathcal{N}(\bar{\mu}_\theta, \sigma_\theta)$ to resample particles as shown in Figure 1(a) where the shaded region A represents the probability of sampling an invalid state. By projecting the invalid states onto the surface of the Bloch sphere, we have essentially sampled the pure state with probability A and used a distribution represented in Figure 1(b). To accommodate the constraints of a valid density matrix without deforming the distribution of the particles and involving further computation required to correct invalid states, we resample using a truncated normal (TN) distribution as shown in Figure 1(c). Sampling procedure for sampling from the probability density function (pdf) of Figure 1(c) is given in Algorithm 1. For each particle, we sample r_k for $k \in \{1, 2, 3\}$ from marginal TN distributions corresponding to X, Y and Z or some other orthogonal axes corresponding to the principal components of the current particle distribution sequentially. We update the domain $[C_1, C_2]$ of the next pdf based on the sample such that the constraint on the Bloch vector $\|\mathbf{r}\| \leq 1$ is not violated. Since we sample from marginal distributions of each axis independently, we must ensure that we can extract marginal pdfs from the available joint pdf. Therefore, we use \mathbf{V} to change the system's bases to the principal components of the existing particle distribution. In this way, we remove existing correlations between

Algorithm 1: Practical resampling for valid states

Input: Particle weights $\{w_k\}$, locations $\{\mathbf{r}_k\}$ for $k \in \{1, \dots, K\}$

Input: $a \in [0, 1]$

Output: Updated weights $\{w'_k\}$, locations $\{\mathbf{r}'_k\}$

```

1  $\boldsymbol{\mu} \leftarrow \text{Mean}(\{w_k\}, \{\mathbf{r}_k\})$ 
2  $h \leftarrow \sqrt{1 - a^2}$ 
3  $\boldsymbol{\Sigma} \leftarrow h^2 \text{Cov}(\{w_k\}, \{\mathbf{r}_k\})$ 
4  $[\mathbf{V}, \boldsymbol{\lambda}] \leftarrow \text{eig}(\boldsymbol{\Sigma})$   $\blacktriangleright \mathbf{V}$  is a matrix of eigenvectors,  $\boldsymbol{\lambda}$  is a vector of eigenvalues
5  $\tau_0 = \tau_1 = \tau_2 = 0$ 
6 for  $k \in 1 \rightarrow K$  do
7   draw  $k^{\text{th}}$  particle  $\mathbf{r}_k$  with probability  $w_k$ 
8    $\boldsymbol{\mu}' \leftarrow \mathbf{V}^T (a\mathbf{r}_k + (1 - a)\boldsymbol{\mu})$   $\blacktriangleright \boldsymbol{\mu}' = (\mu'_0, \mu'_1, \mu'_2)$ 
9   for  $j \in \{0, 1, 2\}$  do
10     $C_1 \leftarrow -\sqrt{1 - \sum_{l=0}^j \tau_l^2}$ 
11     $C_2 \rightarrow -C_1$ 
12     $\tau_j \leftarrow \text{TN}_{[C_1, C_2]}(\mu'_j, \sqrt{\lambda_j})$ 
13    $\mathbf{r}'_k \leftarrow \mathbf{V} \cdot (\tau_0, \tau_1, \tau_2)^T$ 
14    $w'_k \leftarrow 1/K$ 
15 return  $\{w'_k\} \{\mathbf{r}'_k\}$ 

```

bases. Lastly, for each orthogonal axis, we calculate C_1 and C_2 of TN distribution, and sample τ . \mathbf{r}'_k and w'_k are the updated particle's location and weight, respectively.

2.4. Adaptive Bayesian QST

Infidelity scales as $O(1/N)$ when ρ is measured in its own diagonal basis, which is the best possible scaling for QST. However, when this is not the case, it scales as $O(1/\sqrt{N})$ for qubits close to the surface of the Bloch sphere [5],[6]. Since ρ is unknown, the purpose of introducing adaptive protocols is to approach the diagonal basis without losing information gained from intermediary measurement bases. Particle filtering naturally incorporates adaptivity in QST with minimal computational overhead.

The formation of prior is conceptually the first step of our adaptive QST protocol, in that we initially perform measurements on ρ using Pauli operators, and estimate a state, $\hat{\rho}$. We then proceed to change the measurement configuration for the next set of measurements. We use the eigenbases of $\hat{\rho}$ to rotate Pauli X, Y and Z such that the updated operators Ω_1 , Ω_2 and Ω_3 maintain $\text{Tr}(\Omega_i^\dagger \Omega_j) = \delta_{ij}$ and one of the operators diagonalizes $\hat{\rho}$. The particle filter updates the existing distribution based on the outcomes of the measurements in this configuration. We estimate an updated $\hat{\rho}$ and repeat the process iteratively until we have exhausted N or some other criterion is met.

This iterative process is analogous to rotating the plane of measurement (in a two-dimensional space) and cube (in a three-dimensional space) such that the true state

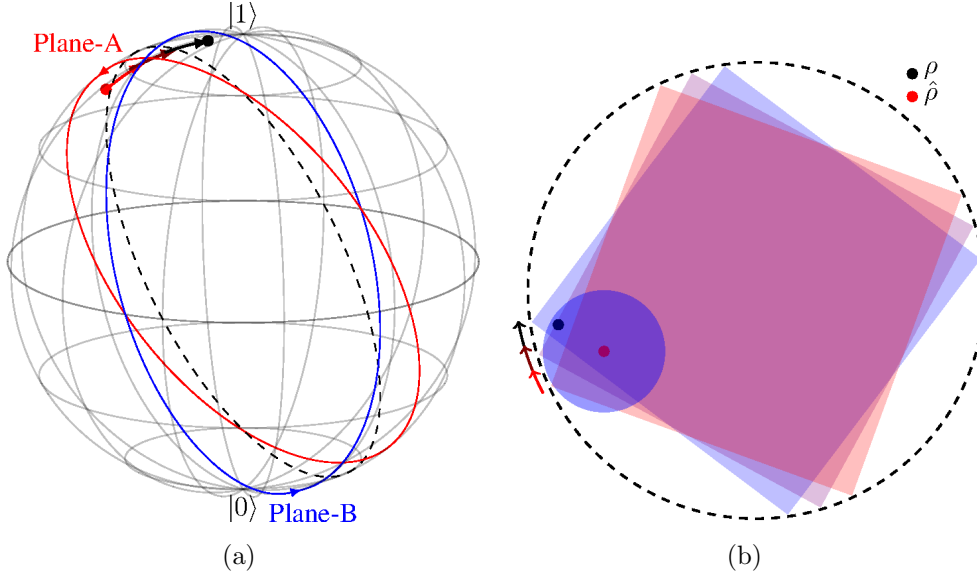


Figure 2. (a) Rotation of planes inside Bloch sphere based on estimated $\hat{\rho}$ where on average the plane move towards ρ with increasing number of iterations. (b) Opposite vertices of inscribed squares represent eigenstates of measurement operators where the adaptive scheme rotates the square such that it moves closer and eventually encompasses the true state to improve scaling of QST.

eventually lies within it, as shown in Figure 2, to achieve the best possible scaling of infidelity. The circular plane represented by a dashed line on the left in Figure 2 is observed in the same figure on the right. The opposite corners of the squares circumscribed by the circle represent the eigenstates of the measurement operators. At a certain step in QST, state $\hat{\rho}$ is approximated. The plane of measurement is rotated such that eigenbases of one of the operators diagonalizes $\hat{\rho}$. The next set of measurements are performed in this configuration, and based on the outcomes a new plane of measurement is selected. The iterative rotation is indicated by the color of the planes in the direction corresponding to the arrows. States close to the surface of the Bloch sphere require a greater number of iterations.

3. Numerical and Experimental Results

In this section, we demonstrate the performance of our protocol detailed in Section 2. We perform QST using open-source packages Qinfer [19] and Qutip [20] on pure and mixed states using our adaptive protocol, and compare the results to non-adaptive PF algorithm. Moreover, we also perform QST on IBM quantum experience [12] to show the readily applicable nature of our work. We report infidelity \mathcal{I} between the estimated states $\hat{\rho}$ and true states ρ defined as [21]

$$\mathcal{I}(\rho, \hat{\rho}) = 1 - \sqrt{\text{tr}(\sqrt{\rho}\hat{\rho}\sqrt{\rho})}. \quad (7)$$

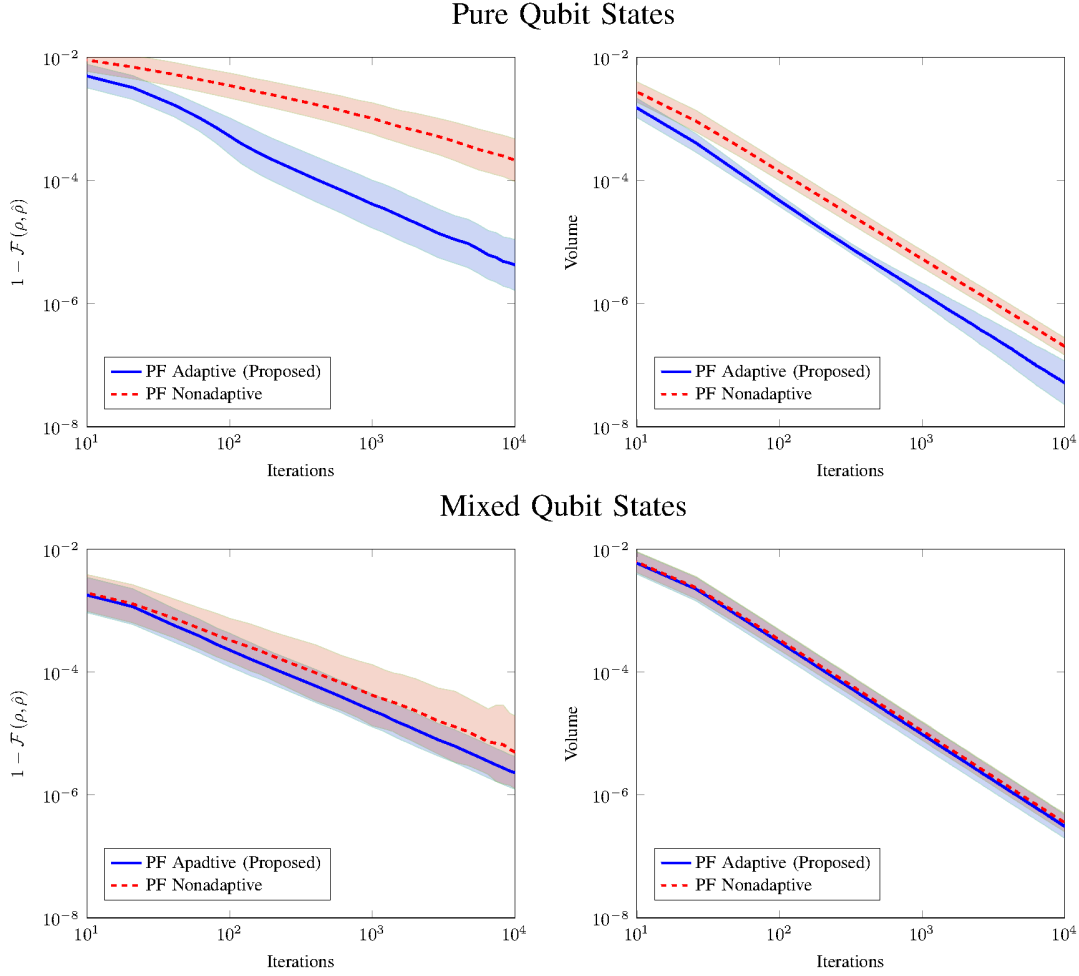


Figure 3. Infidelity and minimum volume enclosing ellipsoid (MVEE) for 99% credible region for the proposed adaptive protocol and its non-adaptive version for pure and mixed states using the method detailed in Section 2 averaged over 1000 particles with the resampling parameter $a = 0.1$. The shaded region indicates the 16% and 84% quantiles over all measurements.

The infidelity captures the idea of closeness between ρ and $\hat{\rho}$ such that $\mathcal{I}(\rho, \hat{\rho}) = 0$ if and only if $\rho = \hat{\rho}$. We also report volumes of covariance Σ -based ellipsoids enclosing 99% credible regions defined as [9], [22]

$$\text{Vol}(\Sigma) = \frac{\pi^{(d-1)/2}}{\Gamma(\frac{d}{2} + 1)} \det(\Sigma)^{-1/2}, \quad (8)$$

where d is the dimension of Σ and Γ is the Gamma function for our simulations and experiments. This measure specifies the concentration of particles by calculating the volume enclosed by a fixed percentage of particles. Thereby helping us gauge the quality of convergence in successive iterations.

Figure 3 demonstrates the advantage of proposed adaptive scheme as compared to non-adaptive PF-based scheme, both in terms of infidelity and the volume for 99% credible regions. The difference between the two schemes is more pronounced for pure

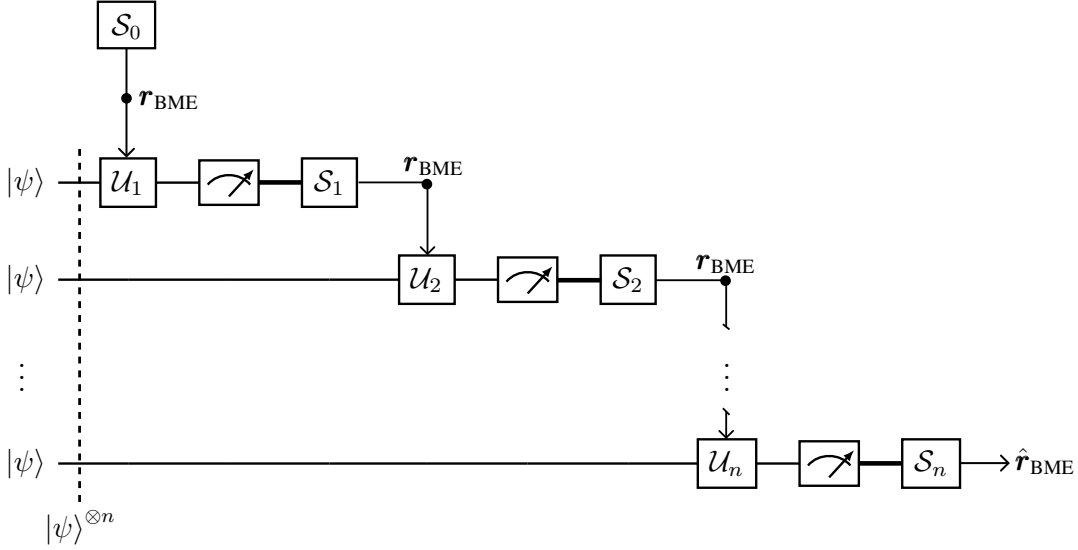


Figure 4. The PF Adaptive QST for single-qubit state $|\psi\rangle$. The \mathcal{U}_{i+1} gate is configured based on the \mathbf{r}_{BME} of PF distribution \mathcal{S}_i at iteration i . \mathcal{U}_{i+1} changes the basis of measurement, and \mathcal{S}_{i+1} is updated based on the measurements counts. The process is initialized with our prior $\mathcal{S}_0 = \mathcal{N}(\boldsymbol{\mu}, \boldsymbol{\Sigma})$, and $\hat{\mathbf{r}}_{\text{BME}}$ is the Bloch vector of our estimate.

states because of the presence of only a single eigenvalue, which reduces uncertainty in measurement in an adaptive setting when the measurement operator diagonalizes a $\hat{\rho}$ that is close to ρ .

To perform QST on a mixed state on IBM’s quantum computer [23], we first prepare a two-qubit pure state $|\psi\rangle = \frac{1}{2} [1, 0, 0, \sqrt{3}] \in H_A \otimes H_B$ so that by taking the partial trace of $|\psi\rangle\langle\psi|$ with respect to Hilbert space H_B , we attain $\rho \in H_A$ defined by the density matrix $\rho = 0.25 |0\rangle\langle 0| + 0.75 |1\rangle\langle 1|$. At any specific iteration, we calculate the weighted aggregate \mathbf{r}_{BME} of the particle distribution to estimate $\hat{\rho}$, and rotate our measurement operators using the unitary operator \mathcal{U} as detailed in Section 2 and demonstrated by the quantum circuit flow diagram in Figure 4. We measure the first qubit and update our particle filter accordingly. We also execute this process for a pure state, and report infidelity \mathcal{I} for both states in Figure 5 for 15 iterations of 1000 shots each.

The infidelity in the experimental implementation drops quickly for initial iterations, i.e., up to 5th iteration for pure and 8th iteration for mixed states. Improvement in later iterations is small, which is a typical behavior of tomography experiments on noisy systems [24]. To obtain these results, we also utilized the noise mitigation offered by QISKIT module to reduce noise from quantum circuits and measurements that increased the number of measurements by a polynomial factor.

4. Discussion

Given that we set out to demonstrate that our method is adept at QST regardless of the purity of the state, we now show its advantage over other contemporary Bayesian

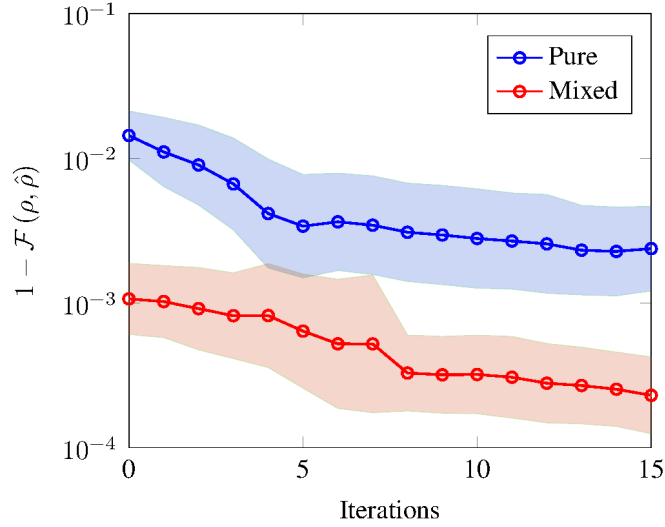


Figure 5. Infidelity of pure and mixed states from measurements on IBM quantum computers averaged over 50 states. Each iteration consists of 1000 shots where fidelity at 0th iteration is due to the prior which performs 3 iterations of 1000 shots along each Pauli axis. The shaded area corresponds to ± 1 standard deviation.

methods. Self-guided quantum tomography (SGQT) is a method that learns pure states through ‘Simultaneous Perturbation Stochastic Approximation’ (SPSA) [10]. However, it does not report error bars and works poorly for mixed states. Practical adaptive quantum tomography (PAQT) [11] is a more rounded technique that builds on SGQT by applying measurements learned by SGQT on a Bayesian particle filter. PAQT can therefore report error bars, and estimate both pure and mixed states. In the process of making a unified technique, PAQT compromises on the infidelities reported by SGQT for pure states. In Figure 6, we demonstrate the median infidelities of SGQT, PAQT and our method for both one qubit pure and mixed states against the number of measurements N . Although, SGQT and our protocol estimates ρ equally well for pure states, our advantage over both techniques is visible when we compare their performance for states of arbitrary purity.

We have also provided a quantum circuit that works hybridly with our particle filter. Although it estimates ρ to a fair extent, it would be best if it is taken as only a proof of concept. The circuit in Figure 5(a) uses the simplest techniques to prepare ρ and rotate measurement operators. More efficient circuits can be used that reduce the decoherence of the prepared state and in turn help us improve our estimates of the true state [25]. Moreover, this technique applies a new measurement in each iteration. Although this requirement is fundamental for initial iterations, more attention can be afforded to its actual efficacy later on. If we can know that after certain n iterations, QST estimates $\hat{\rho}_n$ with measurement configuration k and after $n + 1$ it estimates $\hat{\rho}_{n+1}$ with measurement configuration $k + 1$ where the trace distance $\delta(\hat{\rho}_n, \hat{\rho}_{n+1}) \approx 0$, the computational overhead in calculating and changing to configuration $k + 1$ can be avoided without significant difference to the scaling of our estimate.

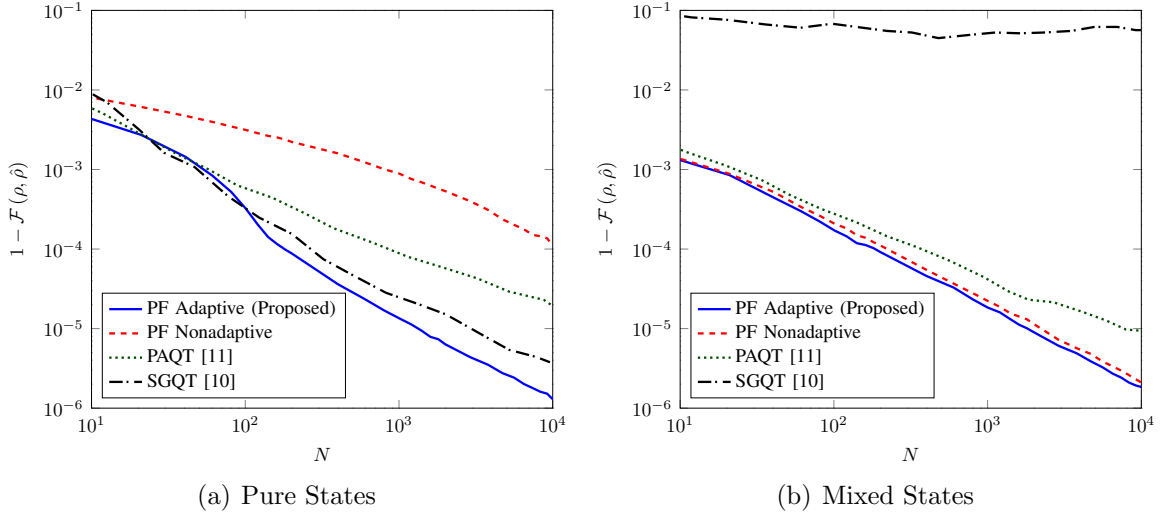


Figure 6. Comparison of median infidelity of pure and mixed state estimations based on proposed protocol, SGQT and PAQT. Each iteration consists of 50 shots along a measurement axis defined by the protocols. The remaining graphs have been translated to accommodate qubits measured for our prior.

5. Conclusion

We proposed an adaptive Bayesian QST technique for qubits that changes the measurement basis in each iteration such that it seamlessly uses the prior as an effective first step. We have reported the numerical and experimental infidelities in our estimates and their uncertainties for arbitrary single qubits. Furthermore, we have provided a comparison of infidelities with popular Bayesian particle filter methods used for QST and demonstrated our advantage in estimation over them. Future work can be done to extend the use of this method for QST of higher dimensions. Another prospective work can be to use the empirically derived prior to produce novel adaptive quantum tomography methods which take advantage of the maximum possible L1 error of the first approximated state.

Acknowledgment

We acknowledge use of the IBM Q for this work. The views expressed are those of the authors and do not reflect the official policy or position of IBM or the IBM Q team. This work was supported by the National Research Foundation of Korea (NRF) grant funded by the Korea government (MSIT) (No. 2019R1A2C2007037).

References

- [1] P. Raynal, X. Lü, and B.-G. Englert, “Mutually unbiased bases in six dimensions: The four most distant bases,” *Phys. Rev. A*, vol. 83, no. 6, p. 062303, 2011.
- [2] F. Yan, M. Yang, and Z.-L. Cao, “Optimal reconstruction of the states in qutrit systems,” *Phys. Rev. A*, vol. 82, no. 4, p. 044102, 2010.

- [3] R. Adamson and A. M. Steinberg, “Improving quantum state estimation with mutually unbiased bases,” *Phys. Rev. Lett.*, vol. 105, no. 3, p. 030406, 2010.
- [4] F. Huszár and N. M. Houlsby, “Adaptive Bayesian quantum tomography,” *Phys. Rev. A*, vol. 85, no. 5, p. 052120, 2012.
- [5] L. Pereira, L. Zambrano, J. Cortés-Vega, S. Niklitschek, and A. Delgado, “Adaptive quantum tomography in high dimensions,” *Phys. Rev. A*, vol. 98, no. 1, p. 012339, 2018.
- [6] D. H. Mahler, L. A. Rozema, A. Darabi, C. Ferrie, R. Blume-Kohout, and A. Steinberg, “Adaptive quantum state tomography improves accuracy quadratically,” *Phys. Rev. Lett.*, vol. 111, no. 18, p. 183601, 2013.
- [7] Blume-Kohout and Robin, “Optimal, reliable estimation of quantum states,” *New J. Phys.*, vol. 12, no. 4, p. 043034, 2010.
- [8] B. Lambert, *A Student’s Guide to Bayesian Statistics*. London: SAGE, 2018.
- [9] C. Ferrie, “High posterior density ellipsoids of quantum states,” *New J. Phys.*, vol. 16, no. 2, p. 023006, 2014.
- [10] —, “Self-guided quantum tomography,” *Phys. Rev. Lett.*, vol. 113, no. 19, p. 190404, 2014.
- [11] C. Granade, C. Ferrie, and S. T. Flammia, “Practical adaptive quantum tomography,” *New J. Phys.*, vol. 19, no. 11, p. 113017, 2017.
- [12] H. Abraham *et al.*, “Qiskit: An Open-source Framework for Quantum Computing,” 2019.
- [13] W. Munro, D. James, A. White, and P. Kwiat, “Measurement of qubits,” *Phys. Rev. A*, vol. 64, no. 030302, 2001.
- [14] A. Doucet, S. Godsill, and C. Andrieu, *On sequential Monte Carlo sampling methods for Bayesian filtering*, 2000, vol. 10, no. 3.
- [15] J. Liu and M. West, *Combined parameter and state estimation in simulation-based filtering*. Springer, 2001.
- [16] C. Granadeand, J. Combes, and D. Cory, “Practical Bayesian tomography,” *New J. Phys.*, vol. 18, no. 3, p. 033024, 2016.
- [17] D. S. Gonçalves, M. A. Gomes-Ruggiero, C. Lavor, O. F. Jiménez, and P. S. Ribeiro, “Local solutions of maximum likelihood estimation in quantum state tomography,” *Quantum Info. Comput.*, vol. 12, no. 9-10, pp. 775–790, 2012.
- [18] P. Bickel, B. Li, T. Bengtsson *et al.*, *Sharp failure rates for the bootstrap particle filter in high dimensions*, 2008.
- [19] C. Granade, C. Ferrie, I. Hincks, S. Casagrande, T. Alexander, J. Gross, M. Kononenko, and Y. Sanders, “Qinfer: Statistical inference software for quantum applications,” *Quantum*, vol. 1, p. 5, 2017.
- [20] J. R. Johansson, P. D. Nation, and F. Nori, “QuTiP: An open-source Python framework for the dynamics of open quantum systems,” *Comput. Phys. Commun.*, vol. 183, no. 8, pp. 1760–1772, 2012.
- [21] M. A. Nielsen and I. L. Chuang, *Quantum Computation and Quantum Information*, 10th ed. New York: Cambridge University Press, 2010.
- [22] C. E. Granade, C. Ferrie, N. Wiebe, and D. G. Cory, “Robust online Hamiltonian learning,” *New J. Phys.*, vol. 14, no. 10, p. 103013, 2012.
- [23] 5-qubit backend: IBM Q team, IBM Q 16 Melbourne backend specification v2.3.1 (2020). Retrieved form (<http://ibm.biz/qiskit-melbourne>). (Accessed: May 2020).
- [24] G. I. Struchalin, I. A. Pogorelov, S. S. Straupe, K. S. Kravtsov, I. V. Radchenko, and S. P. Kulik, “Experimental adaptive quantum tomography of two-qubit states,” *Phys. Rev. A*, vol. 93, no. 1, p. 012103, 2016.
- [25] A. Zulehner, A. Paler, and R. Wille, “An efficient methodology for mapping quantum circuits to the IBM QX architectures,” *IEEE Trans. Comput.-Aided Des. Integr. Circuits Syst.*, vol. 38, no. 7, pp. 1226–1236, 2018.